Biophysical Journal, Volume *115*

Supplemental Information

Architecture-Dependent Anisotropic Hysteresis in Smooth Muscle Cells

Zaw Win, Justin M. Buksa, and Patrick W. Alford

SUPPLEMENTAL MATERIALS AND METHODS

Photolithography to fabricate PDMS stamps. Polydimethylsiloxane (PDMS) stamps were fabricated using common soft photolithography methods (1). Photomasks were designed using AutoCAD software (Autodesk, San Rafael, CA) and printed onto a Mylar film (Fineline Imaging, Colorado Springs, CO). To generate isolated single cell islands for micropatterning, features of aspect ratios (AR) 4, 2, and 1 (AR4: 32 μm x 128 μm, AR2: 91 μm x 44 μm, AR1: 63 μm x 63 μm) were placed in arrays 200 μm apart from other features to prevent crowding of individual features. Silicon masters were fabricated at the Minnesota Nano Center. Briefly, a clean 3.5 in silicon wafer (Wafer World Inc., West Palm Beach, FL) was primed with HMDS vapor for 3 min. Then AZ-9260 photoresist (AZ Electronic Materials USA Corp., Somerville NJ) was coated onto the wafer at 2000 rpm for 60 s (5000 rpm/s acceleration). The wafer was heated to 110 ºC on a hot plate for 165 s. The photomask and photoresist coated wafer were exposed with UV illumination for 3 cycles of 14 s each with a 10 s gap (42 s total duration) at 12 mW/cm^2 using a Karl Suss MA6 contact aligner. After exposure, the wafer was developed in a 1:4 mixture of H_2O:AZ 400k developer solution with gentle agitation for 2.5 min followed by rinsing in distilled water. Sylgard 184 PDMS was used to mold PDMS stamps from the silicon wafer. PDMS stamps were sonicated in 70% ethanol for 30 min then dried prior to use.

CμBS substrate fabrication. Micropatterned CμBS substrates were prepared as previously described (2).

*Membrane preparation***.** Elastomer membranes (0.01 in thick, Specialty Manufacturing, Saginaw, MI) were cut into 30 mm x 30 mm cruciform shapes and placed into custom grips (40 mm grip to grip distance) under tension. Glass slides were adhered to the bottom of the membranes to provide structural support and to prevent oxygen diffusion into the membrane. PDMS rings (30 mm diameter x 3 mm wall thickness) were bonded to the top side of the membrane to serve as a reservoir for cell culture media. Membranes were them treated with 10% w/v benzophenone (Sigma-Aldrich, St. Louis, MO) dissolved in a 70:30 solution of acetone:water for 1 min. The membranes were then rinsed with methanol and degassed in a vacuum aspirator for 30 min prior to gel polymerization.

Micropatterning. Clean PDMS stamps were incubated with 100 μg/mL of fibronectin (BD Biosciences, San Jose, CA) for 1 h then blown dry with air. O_2 plasma treated glass coverslips

were then stamped with fibronectin-coated stamps and held in conformal contact for 30 min at room temperature.

Gel polymerization. Pre-polymer solution consisting of 625 μL 40% acrylamide (Sigma-Aldrich), 163 μL 2% bis-acrylamide (Sigma-Aldrich), 25 μL of 5 mg/mL acrylic acid N-hydrosuccimide ester, 35 μL 1 M HCl, and 25 μL fluorescent beads (0.2 μm red beads, 2% solids, Polysciences, Warrington, PA) was prepared and degassed for 30 min. Initiators tetramethylethylenediamine (5 μL) and 12.5 μL 10% w/v ammonium persulfate were added to the pre-polymer solution and 10 μL of the solution was deposited onto a benzophenone-functionalized elastomer substrate. The micropatterned glass coverslip was placed on the pre-polymer solution and exposed to UV illuminator in a Jelight 342 UVO cleaner for 30 min approximately 2.5 cm distance from the lamp to initiate polymerization. After gel polymerization and micropattern transfer from the coverglass to the gel, the constructs were hydrated in water for 15 min. The coverglass was peeled from the top of the gel and the glass slide was removed from the membrane. The gels were incubated in 4% bovine serum albumin in PBS to inactivate unreacted acrylic acid N-hydrosuccinimide ester. After inactivation, CμBS substrates were incubated in PBS for 48-72 h to remove residual benzophenone and unreacted pre-polymer constituents prior to cell seeding.

Cell culture. Human umbilical artery smooth muscle cells (VSMCs) were obtained from Lonza (Walkersville, MD) at passage 3 and only passages 4-7 were used for experiments. VSMCs were cultured at 37 ºC and 5% CO_2 in growth medium consisting of Medium 199 (GenDEPOT, Baker, TX) supplemented with 10% heat-inactivated fetal bovine serum (Gibco, Grand Island, NY), 10 mM HEPES (Gibco), 3.5 g L^{-1} glucose (Sigma-Aldrich), 2 mg L^{-1} vitamin B12 (Sigma-Aldrich), 50 U mL^{-1} penicillin-streptomycin (Gibco), 1x MEM non-essential amino acids (Gibco), and 2 mM L-glutamine (Gibco). Cells were seeded at 10,000-20,000 cells per construct overnight in growth medium. After overnight adherence, cells were serum starved in serum free media for 24-48 h prior experiments to induce a physiological phenotype (3).

Cell structure measurements. Cells were fixed using 4% paraformaldehyde (Electron Microscopy Sciences, Hatfield, PA) for 5 min then stained for F-actin (Alexa Fluor 488 Phalloidin, Life Technologies, Eugene, OR). F-actin stacks (0.45 μm/slice, 20 slices) were obtained used an Olympus FluoView FV1000 BX2 laser scanning microscope (UPlanFLN, 40X, NA 1.30), at the University Imaging Centers, University of Minnesota. A custom Matlab script was used to determine average cell thicknesses to create cell thickness maps over the adhered

area of the cell. Cell cross-section area was determined by integrating the cell thickness where axial cross-sectional area (A_x) was taken as the mean area over the middle 50% of the cell along the length (x-direction) and transverse cross-sectional area (A_y) was taken as the mean area over the middle 50% of the cell along the width (y-direction).

Fiber distributions measured from 2D projections of F-actin confocal stacks were fit to a von Mises distribution function of the form

$$f(\theta;\kappa,\theta_p) = \frac{e^{\kappa\cos[2(\theta-\theta_p)]}}{\pi I_0(\kappa)} \qquad [1]$$

where κ is the fiber concentration factor, describing the spread of the fiber distribution around preferred orientation θ_p and $I_0(\kappa)$ is the modified Bessel function of the first kind of order 0 where,

$$I_n(\kappa) = \frac{1}{\pi}\int_0^{\pi} e^{\kappa\cos(\theta)}\cos(n\theta)\,d\theta \qquad [2]$$

Cell stretching. Stretching experiments (Fig S1B,C) were conducted inside a temperature controlled environmental chamber at 37 °C on an Olympus X-81 inverted microscope at 40x magnification (UPLSAPO40X2, NA 0.95). The constructs were removed from the incubator immediately prior to stretching experiments and serum free media was replaced with 2 mL of Tyrode's buffer. Cell-seeded CμBS substrates were placed into the CμBS device (Fig S1A) then exposed to either uniaxial or equibiaxial stretching protocols to 25% grip strain for uniaxial or 20% grip strain for equibiaxial stretches. First, a priming stretch identical to the experimental stretch (uniaxial or equibiaxial) was performed. 3-5 cells were identified to be measured. Then cell locations were saved to Metamorph Image Acquisition software. The substrate was stretched in increments up 5% grip strain up to the maximum prescribed strain. Displaced cell positions were tracked manually and saved to the software at each step. Active cell stretch was performed by increments of 5% loading strain (0.1%/s ramp rate) to the substrate with 2 min hold periods where a brightfield image of the cell and fluorescent image of the beads in the top layer of the gel nearest to the cell were taken at each step. After reaching the maximal prescribed loading strain (25% uniaxial, 20% eqiubiaxial), cells were unloaded by performing -5% unloading strain to the substrate while acquiring images in the same manner as loading strain. After a full cycle of load-unload, cells were passivated with 100 μM of HA-1077 for 1 h. A full load-unload cycle was repeated on the passive cells and data required at each increment of

5% grip strain. NucBlue reagent (ThermoFisher, Waltham, MA) was used to verify micropatterned cells only had one nuclei. Finally, cells were lysed with 0.5% sodium dodecyl sulfate and the stretching protocol was repeated to acquire cell-free deformation of beads. Substrate deformations due to applied grip strains were calibrated by measuring displacement of beads during cell-free deformation of the substrate. Substrate stretch ratios, λ_x and λ_y, were taken as the measured cell-free substrate deformations.

1. Xia, Y., and G. M. Whitesides. 2003. Soft Lithography. Angewandte Chemie 37(5):550-575. review-article.
2. Win, Z., J. M. Buksa, K. E. Steucke, G. W. Gant Luxton, V. H. Barocas, and P. W. Alford. 2017. Cellular Microbiaxial Stretching to Measure a Single-Cell Strain Energy Density Function. Journal of biomechanical engineering 139(7).
3. Han, M., J. K. Wen, B. Zheng, Y. Cheng, and C. Zhang. 2006. Serum deprivation results in redifferentiation of human umbilical vascular smooth muscle cells. American Journal of Cell Physiology 291(1):C50-58.

SUPPLEMENTAL FIGURES

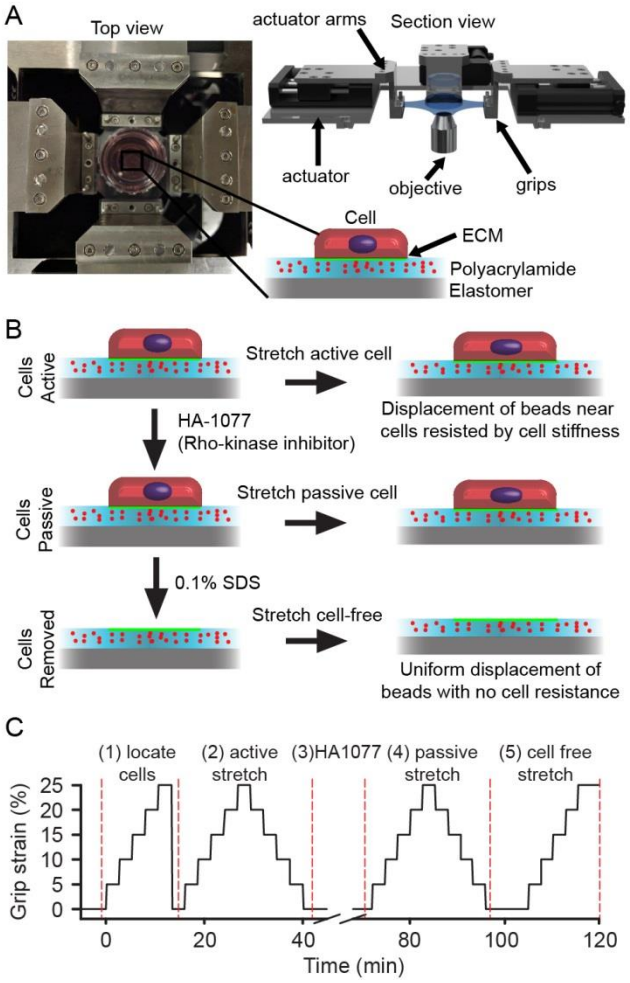

Figure S1. Cellular micro-biaxial stretching (CμBS) method to measure active and passive cell stress. (A) Schematic of CμBS device and substrate. Top view: photograph of substrate mounted in device. Inset: Micropatterned cell polyacrylamide-elastomer substrate. Side view: Rendered image of device. (B) Stretch protocol to measure substrate bead displacements in active and passive cells. (C) Time course of stretch protocol to stretch active and passive cells.

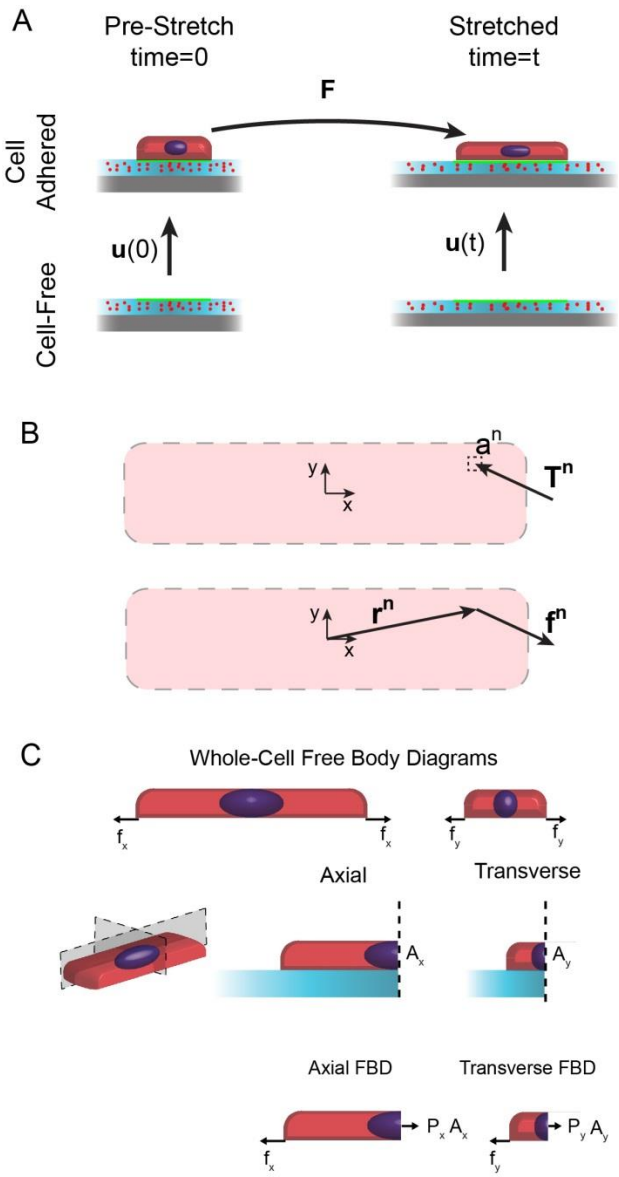

Figure S2. Methods for measuring cell stress (A) Cell and substrate deformation. Deformation gradient tensor $\boldsymbol{F}$ represents the deformation from the pre-stretched to the stretched state. Cell-induced substrate displacement $\boldsymbol{u}$ is the defomation of the substrate caused by the cell, which is determined by comparing the substrate position in the cell-adhered and cell-free states. (B) Surface traction and cell force. Top: substrate surface traction stress $\boldsymbol{T^n}$ acting on face a^n. Bottom: cell force $\boldsymbol{f^n} = \boldsymbol{T^n} a^n$ located at position $\boldsymbol{r^n}$, relative to the center of the cell. (C) Cell cross-sections and force balances. Top: Free body diagrams for whole-cell equilibrium. Middle: Cell subdivided to determine cell mid-plane cross-sectional areas A_x and A_y. Bottom: Free body diagram used to determine mid-plane stresses. Note: moments are considered negligible.

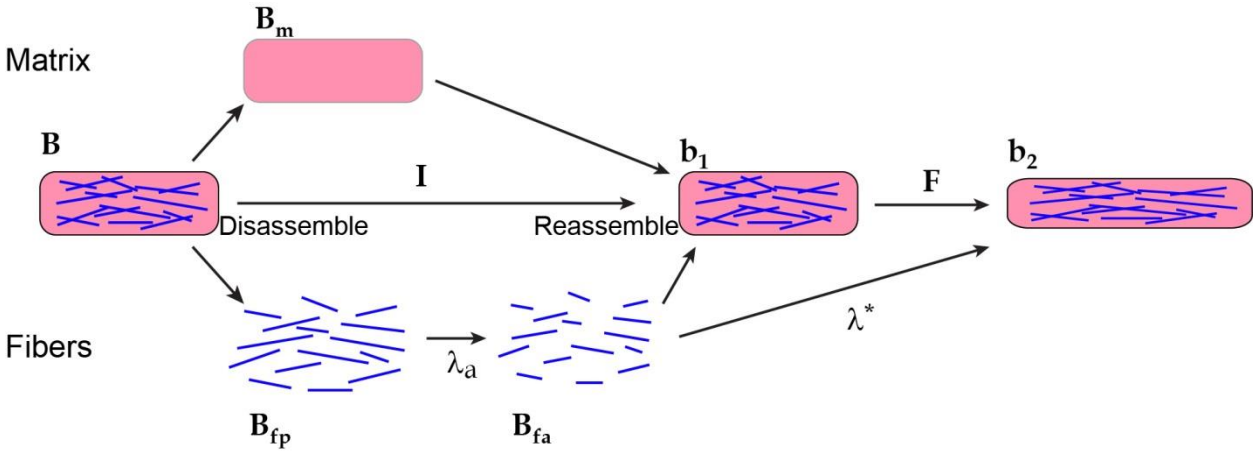

Figure S3. Configurations for fiber contraction and deformation. Stress-free configuration denoted by capital $B's$. Stressed configurations denoted by lower case $b's$.

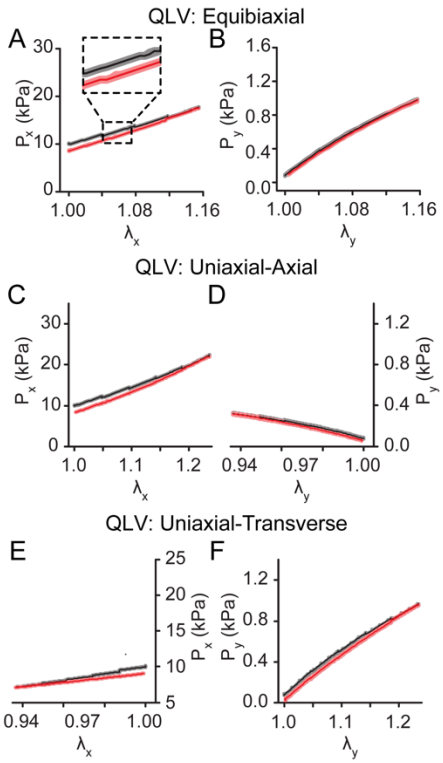

Figure S4. Anisotropic hysteresis is not well-described by a quasilinear viscoelastic model (A-B) QLV model for equibiaxial stretch, fit to experimental data during. (A) Model-predicted axial cell stresses (P_x) during equibiaxial stretch. Inset: enlarged image of plot showing mean stresses (dark line) and 95% confidence interval (shaded) calculated with 100 runs. (B) Model-predicted transverse cell stresses (P_y) during equibiaxial stretch. (C-D) QLV model for uniaxial-axial stretch, using parameters fit to equibiaxial data. (C) Model-predicted axial cell stresses (P_x) during uniaxial-axial stretch. (D) Model-predicted transverse cell stresses (P_y) during uniaxial-axial stretch. (E-F) QLV model for uniaxial-tansverse stretch, using parameters fit to equibiaxial data. (E) Model-predicted axial cell stresses (P_x) during uniaxial-transverse stretch. (F) Model-predicted transverse cell stresses (P_y) during uniaxial-transverse stretch. For all figures: Black: loading. Red: unloading.

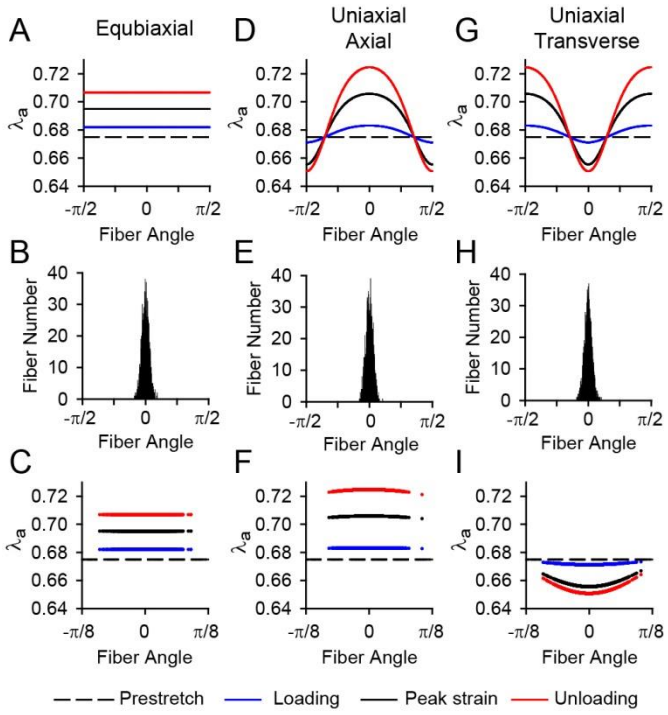

Figure S5. Orientation-dependent model-predicted individual fiber contraction. (A) Equibiaxial fiber angle-dependent active stretch ratios (λ_a) at the midpoint of the hold phase of $\lambda_x = \lambda_y = 1.08$ during loading (blue), $\lambda_x = \lambda_y = 1.16$ (black), and $\lambda_x = \lambda_y = 1.08$ during unloading (red). (B) Representative histogram of fiber angles used in model. (C) Active stretch ratios (λ_a) for all fibers from (B) in the equibiaxial model at the timepoints in (A). (D) Uniaxial-axial fiber angle-dependent active stretch ratios (λ_a) at the midpoint of the hold phase of $\lambda_x = 1.09$ during loading (blue), $\lambda_x = 1.225$ (black), and $\lambda_x = 1.09$ during unloading (red). (E) Representative histogram of fiber angles used in model. (F) Active stretch ratios (λ_a) for all fibers from (E) in the uniaixial-axial model at the timepoints in (D). (G) Uniaxial-transverse fiber angle-dependent active stretch ratios (λ_a) at the midpoint of the hold phase of $\lambda_x = 1.09$ during loading (blue), $\lambda_x = 1.225$ (black), and $\lambda_x = 1.09$ during unloading (red). (H) Representative histogram of fiber angles used in model. (I) Active stretch ratios (λ_a) for all fibers from (H) in the uniaixial-transverse model at the timepoints in (G).

Supplemental Table 1. QLV model parameter values

Parameter	Value
μ	1.5 kPa
C_f	2.25 kPa
λ_{a0}	0.61
α	0.875
β	0.125